J. Inverse Ill-Posed Probl. Galley Proof, 13 pages
DOI 10.1515/jip-2012-0052

Inverse determination of unsteady temperatures and heat fluxes on inaccessible boundaries

Brian H. Dennis and George S. Dulikravich

Abstract. The direct measurement of temperatures and heat fluxes may be difficult or impossible on boundaries that are inaccessible, such as internal cavities, or exposed to harsh environmental conditions that would destroy the thermal sensors. In such circumstances, one may inversely determine the temperature and heat fluxes on these unknown boundaries by using over-specified conditions on boundaries where such information can be readily collected. This assumes the geometry and material properties of the domain are known. Algorithms for solving these problems, such as those based on finite difference, finite element, and boundary element, are well known for the case where measured boundary conditions are not a function of time. In this work, we demonstrate an inverse finite element method that effectively solves this inverse heat conduction problem using over-specified temperatures and heat fluxes that are time varying. The material properties may be highly heterogeneous and non-linear. A boundary regularization method is used to stabilize the method for cases involving errors in temperature and heat flux measurements. Several three-dimensional examples are given using simulated measurements with and without measurement errors, to demonstrate the accuracy of the method.

Keywords. Inverse problems, heat conduction, finite element method, regularization.

2010 Mathematics Subject Classification. 80.

1 Introduction

Many practical engineering applications require monitoring of surface temperatures and heat fluxes, but in some situations it may be difficult and even impossible to place probes on the desired surface of a solid body. This can be either due to its small size, geometric inaccessibility, or because of exposure to a hostile environment that may destroy the probe. With an appropriate inverse method, these unknown boundary values on the desired surface can be deduced from additional information available at a finite number of points within the body and/or on some other surfaces of the solid body. In the case of heat conduction, the objective of an inverse boundary condition determination problem is to compute the temperatures and heat fluxes on any surfaces or surface elements where such information is unknown [1].

Note 1: Please supply MSC 2010

The inverse approach for determining unknown boundary conditions in heat conduction is a well-studied problem for steady heat conduction in simplified domains with linear materials [1, 3–6, 8].

However, many real world applications involve complex geometries with nonlinear and heterogeneous material properties and require the determination of unsteady temperature boundary conditions.

For inverse problems, the unknown boundary conditions on parts of the boundary can be determined by overspecifying the boundary conditions (enforcing both Dirichlet and Neumann type boundary conditions) on at least some of the remaining portions of the boundary, and providing either Dirichlet or Neumann type boundary conditions on the rest of the boundary. It is possible, after a series of algebraic manipulations, to transform the original system of equations into a system which enforces the overspecified boundary conditions and includes the unknown boundary conditions as a part of the unknown solution vector. This approach has been used successfully for steady heat conduction [1,3,6]. In this paper, we present the extension of this method to unsteady heat conduction problems.

2 FEM formulation for heat conduction

The temperature field distribution throughout the domain can be found by solving the heat equation for unsteady thermal conduction (2.1). The material properties may be spatially varying and may depend on temperature. The density, ρ, specific heat capacity, Cp, and thermal conductivity coefficient, k, as well as the objects' geometry are assumed to be known. The effect of heat sources and sinks, such as latent heats due to chemical reactions or phase changes or Joule heatings, can be incorporated with a distributed heat source function, S. We note that these quantities may be functions of time, space, and temperature,

$$\rho Cp \frac{\partial T}{\partial t} - \nabla \cdot (k \nabla T) = S. \tag{2.1}$$

Applying the method of weighted residuals to (2.1) over an element results in the following functional equation:

$$\pi = \int_{\Omega^e} v \left(\rho Cp \frac{\partial T}{\partial t} - \nabla \cdot (k \nabla T) - S \right) d\Omega^e \tag{2.2}$$

where v is a non-zero weight function. Integrating (2.2) by parts once reduces the required continuity for functions representing T over each element and eliminates the need to differentiate the $k\nabla T$ product,

$$\pi = \int_{\Omega^e} v \rho Cp \frac{\partial T}{\partial t} \, d\Omega^e - \int_{\Omega^e} k \nabla v \cdot \nabla T \, d\Omega^e - \int_{\Omega^e} vS \, d\Omega^e + \int_{\Gamma^e} v(\vec{q} \cdot \vec{n}) \, d\Gamma^e. \tag{2.3}$$

Variation of the temperature and the weight function across an element with m nodes can be expressed by

$$T^e(x,y,z) = \sum_{i=1}^{m} N_i(x,y,z) T_i^e = \{N\}^T \{T^e\}, \tag{2.4}$$

$$v^e(x,y,z) = \sum_{i=1}^{m} N_i(x,y,z) v_i^e = \{N\}^T \{v^e\} \tag{2.5}$$

where the functions N_i for v^e and T^e are chosen to be the same. The functions v^e and T^e are substituted into (2.3) leading to a discrete weak statement. The discrete weak statement functional is then made stationary with respect to the weight function coefficients v_i resulting in a system of non-linear ordinary equations for the element. These equations can be expressed in matrix form as

$$[C^e]\{\dot{T}^e\} + [K^e]\{T^e\} = \{Q^e\} \tag{2.6}$$

where

$$[C^e] = \int_{\Omega^e} \rho Cp \{N\}\{N\}^T \, d\Omega^e, \tag{2.7}$$

$$[K^e] = \int_{\Omega^e} k [B]^T [B] \, d\Omega^e, \tag{2.8}$$

$$[B] = \begin{bmatrix} \frac{\partial N_1}{\partial x} & \frac{\partial N_2}{\partial x} & \cdots & \frac{\partial N_m}{\partial x} \\ \frac{\partial N_1}{\partial y} & \frac{\partial N_2}{\partial y} & \cdots & \frac{\partial N_m}{\partial y} \\ \frac{\partial N_1}{\partial z} & \frac{\partial N_2}{\partial z} & \cdots & \frac{\partial N_m}{\partial z} \end{bmatrix}, \tag{2.9}$$

$$\{Q^e\} = -\int_{\Omega^e} S\{N\} \, d\Omega + \int_{\Gamma^e} q_s \{N\} \, d\Gamma^e. \tag{2.10}$$

The time derivative is then discretized using a straightforward θ-method time marching approach resulting in (2.11). In addition, the system can be linearized using values of k, Cp, ρ, and S from the previous time step or iteration. Alternatively, inner iteration using Picard's or Newton's method each time step can be used to linearize the system. Our previous experience has shown that these heat conduction problems are not highly non-linear and require only a few iterations to converge each time step. In most cases, linearization in time without inner iteration is sufficient

$$\begin{aligned} &\left(\frac{[C^e(T^n)]}{\Delta t} + \theta [K^e(T^n)] \right) \{T^{n+1}\} \\ &\quad = \{Q^e\} + \left(\frac{[C^e(T^n)]}{\Delta t} + (\theta - 1)[K^e(T^n)] \right) \{T^n\}. \end{aligned} \tag{2.11}$$

The value of θ dictates whether the scheme is implicit or explicit, and first or second order accurate in time. We use $0.5 \le \theta \le 1.0$ for both forward and inverse analysis, thus requiring the simultaneous solution of the system of equations each time step. This approach requires knowledge of the initial temperature to start the marching process.

The element matrices and vectors are determined for each element in the domain and then assembled into the global system of linear algebraic equations

$$[K(T^n)]\{T^{n+1}\} = \{Q(T^n)\}. \tag{2.12}$$

This system is solved each time step for both forward and inverse problems. Both require knowledge of the boundary and initial conditions to start the time marching process.

3 Direct and inverse formulations

The above equations for unsteady heat conduction were discretized by using a Galerkin finite element method. The system is typically large, sparse, symmetric, and positive definite. Once the global system has been formed, the boundary conditions are applied. For a well-posed analysis (forward) problem, the boundary conditions must be known on all boundaries of the domain. For heat conduction, either the temperature, T_s, or the heat flux, Q_s, must be specified at each point of the boundary.

Here we use series of algebraic manipulations to transform the original system of linear equations into an alternate system that represents the inverse problem. The modified system enforces the over-specified boundary conditions while including the unknown boundary conditions as a part of the unknown solution vector. As an example, consider the linear system for heat conduction on a tetrahedral finite element with boundary conditions given at nodes 1 and 4

$$\begin{bmatrix} K_{11} & K_{12} & K_{13} & K_{14} \\ K_{21} & K_{22} & K_{23} & K_{24} \\ K_{31} & K_{32} & K_{33} & K_{34} \\ K_{41} & K_{42} & K_{43} & K_{44} \end{bmatrix} \begin{Bmatrix} T_1 \\ T_2 \\ T_3 \\ T_4 \end{Bmatrix} = \begin{Bmatrix} Q_1 \\ Q_2 \\ Q_3 \\ Q_4 \end{Bmatrix}. \tag{3.1}$$

As an example of an inverse problem, one could specify both the temperature, T_s, and the heat flux, Q_s, at node 1, flux only at nodes 2 and 3, and assume the boundary conditions at node 4 as being unknown. The original system of equations (3.1) can be modified by adding a row and a column corresponding to the additional equation for the over-specified flux at node 1 and the additional unknown due to the unknown boundary flux at node 4

$$\begin{bmatrix} 1 & 0 & 0 & 0 & 0 \\ K_{21} & K_{22} & K_{23} & K_{24} & 0 \\ K_{31} & K_{32} & K_{33} & K_{34} & 0 \\ K_{41} & K_{42} & K_{43} & K_{44} & -1 \\ K_{11} & K_{12} & K_{13} & K_{14} & 0 \end{bmatrix} \begin{Bmatrix} T_1 \\ T_2 \\ T_3 \\ T_4 \\ Q_4 \end{Bmatrix} = \begin{Bmatrix} T_s \\ Q_2 \\ Q_3 \\ 0 \\ Q_s \end{Bmatrix}. \tag{3.2}$$

The resulting systems of equations will remain sparse, but will be unsymmetric and possibly rectangular depending on the ratio of the number of known to unknown boundary conditions. We note that this procedure is repeated each time step for the unsteady inverse analysis.

4 Regularization

It is well known that ill-conditioned problems, such as many inverse problems, are very sensitive to error. The error may come from round-off due to finite precision calculations, or from input data, such as when actual experimental data is used. In either case, introduction of error can cause spurious non-physical results to appear. To make the approach robust against error, we apply a regularization method to the inverse finite element method.

Tikhonov regularization [10] method is the most widely used approach. However, our previous research has shown that higher-order regularization methods result in more accurate solutions to inverse boundary condition problems [1, 3].

The general form of a regularized system is given as (see [7])

Note 2: Red parts indicate major changes. Please check them carefully.

$$\begin{bmatrix} K \\ \Lambda D \end{bmatrix} \{T\} = \begin{Bmatrix} Q \\ 0 \end{Bmatrix} \tag{4.1}$$

where the traditional Tikhonov regularization is obtained when the damping matrix, $[D]$, is set equal to the identity matrix. Solving (4.1) in a least squares sense minimizes the following error function:

$$\text{error}(T) = \|[K]\{T\} - \{Q\}\|_2^2 + \|\Lambda[D]\{T\}\|_2^2. \tag{4.2}$$

This is the minimization of the residual plus a penalty term. The form of the damping matrix determines what penalty is used and the damping parameter, Λ, weights the penalty for each equation. These weights should be determined according to the measurement error associated with the respective equation. The Tikhonov approach clearly drives the solution to zero as the damping parameter increases. For this reason, we avoid using the Tikhonov regularization method in inverse boundary detection problems.

The method used here is essentially a Laplacian smoothing of the unknown temperatures on the boundaries where the boundary conditions are unknown. This method could be considered a "second order" Tikhonov method. A penalty term can be constructed such that curvature of the solution on the unspecified boundary is minimized along with the residual

$$\|\nabla^2 T_{\mathrm{ub}}\|_2^2 \to \min. \tag{4.3}$$

Equation (4.3) is discretized using the method of weighted residuals to determine the damping matrix, $[D]$,

$$\|[D]T_{\mathrm{ub}}\|_2^2 = \|[K]T_{\mathrm{ub}}\|_2^2. \tag{4.4}$$

In three-dimensional problems, $[K]$ is computed by integrating over surface elements on the inaccessible boundaries. So the damping matrix represents an assembly of boundary elements that compose the inaccessible boundary. The stiffness matrix for each boundary element is formed by using a Galerkin weighted residual method that ensures the Laplacian of the solution is minimized over the unknown boundary surface. The main advantage of this method is its ability to smooth the solution vector without necessarily driving the components to zero and away from the true solution.

5 Numerical results

The finite element inverse formulation was shown previously to be both accurate and efficient for several three-dimensional test problems in steady heat conduction [2, 3].

Following a similar approach, the proposed unsteady inverse finite element method was applied to some three-dimensional test problems to demonstrate accuracy of the method.

The method has been implemented in an object-oriented finite element code written in C++. The software uses sparse matrix storage that allows 3-D problems to be solved on a multi-core personal computer in less than a few minutes. Elements used in the calculations were hexahedra with tri-linear interpolation functions.

In general, the resulting FEM systems for inverse finite element problems are sparse, unsymmetric, and often rectangular. These properties make the process of finding a solution to the system very challenging. One possible approach is to use iterative methods suitable for least squares problems. One such method is the

LSQR method [9], which is an extension of the well-known conjugate gradient (CG) method. The LSQR method and other similar methods such as the conjugate gradient for least squares (CGLS) solve the normalized system, but without explicit computation of $[K][K]^T$. These methods need only matrix-vector products at each iteration and therefore only require the storage of the solution vectors if the products are computed on an element-by-element basis. This makes the iterative approach attractive for large sized models. In addition, the matrix-vector product is naturally parallel, and thus is easily applied to massively parallel computing resources. The linear system for the cases shown here are solved with a sparse LSQR solver.

For the first test case, we consider heat conduction in an insulated carbon steel rod with time varying temperature applied on the bottom end. We note that this problem is a relatively simple test case with linear properties, a spatially one-dimensional solution, and has no measurement errors included.

The test geometry and boundary conditions are illustrated in Figure 1. The rod has a length of 50.0 cm and a square cross-section with a width of 10.0 cm. Constant material properties of $\rho = 7800.0\,\text{kg}/m^3$, $Cp = 500.0\,J/\text{kg}\cdot K$, and $k = 40.0\,W/m\cdot K$ were used. The rod was meshed with ten uniformly spaced hexahedral elements.

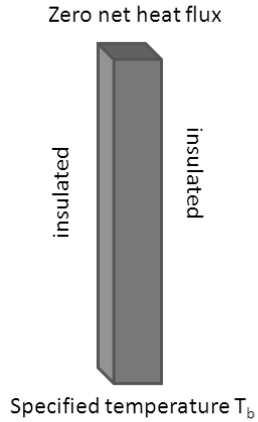

Figure 1. Boundary conditions for rod test problem.

A forward problem was created by specifying an initial condition of

$$T(x,y,z) = 0.0^o C$$

and the boundary condition $T_b = 20.0\sin(2\pi t/10.0) + 50.0$. All other boundaries were insulated. A time step size $\Delta t = 0.5s$ was used. The computed temperature and heat flux on the top of the rod were stored in a file in double precision at each time step. This data was then used for simulated measurements for the inverse test problem discussed below.

For the inverse problem, T_b and the corresponding heat flux are considered unknown, while the simulated measurements obtained from the forward problem were overspecified on the opposite end of the rod. The same geometry, material properties, initial temperature, and time step size used for the forward problem were also used for the inverse case. A damping coefficient $\Lambda = 1.0 \times 10^{-30}$ was used.

Figure 2 compares the results for T_b for the inverse and forward problems. The inverse method predicts temperature that is within 1.0% of the forward solution. More importantly, the error does not appear to grow with time, indicating the method is both accurate and stable for this test case.

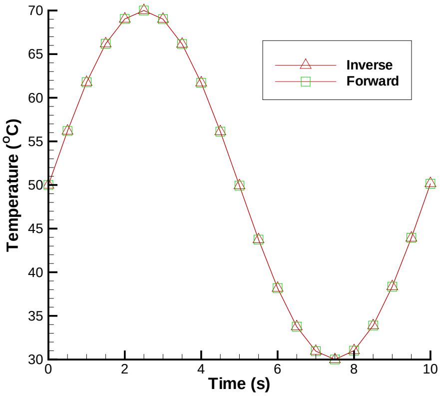

Figure 2. Predicted boundary temperature T_b for forward and inverse cases.

The second test case is a slightly more complex demonstration. This case involves the time varying surface heat flux applied to a three-dimensional plate. The plate geometry and mesh are shown in Figure 3. The mesh is composed of 2116 hexahedral elements. The boundary conditions for the forward problem are shown in Figure 4. The carbon steel plate material has the properties $\rho = 7800.0\,\mathrm{kg}/m^3$, $Cp = 500.0\,J/\mathrm{kg}\cdot K$, $k = 40.0\,W/m\cdot K$.

A time varying temperature function was created to simulate a directed energy beam moving diagonally across the top of the plate as shown in Figure 5. Note that the temperature is non-dimensionalized according to

$$T = 100.0\frac{T_{\mathrm{computed}} - T_{\mathrm{min}}}{T_{\mathrm{max}} - T_{\mathrm{min}}}. \tag{5.1}$$

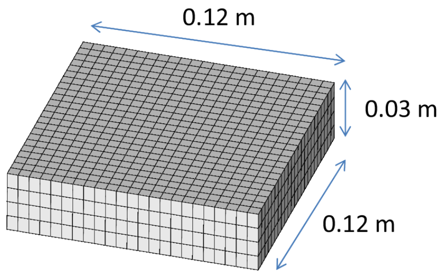

Figure 3. Plate geometry and mesh for second test case.

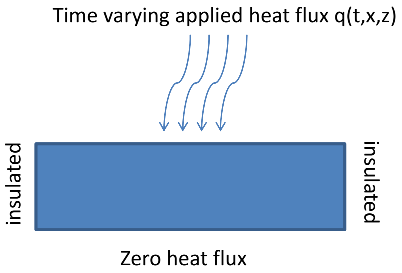

Figure 4. Boundary conditions for second test case forward problem.

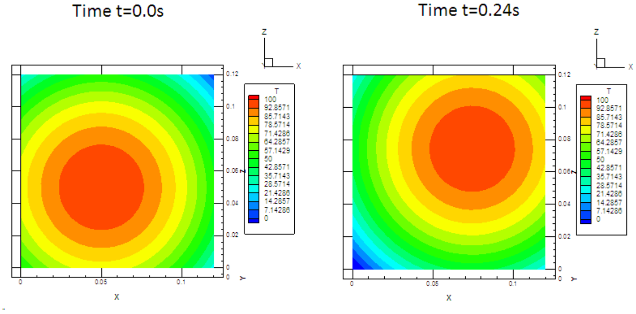

Figure 5. Time varying temperature on the plate top for forward problem.

As in the first case, the forward problem is solved while storing temperatures and fluxes on the bottom surface of the plate. The stored double precision data was then used as simulated measurements for the inverse case. A time step size $\Delta t = 0.012s$ was used for generating these simulated measurements.

The inverse case was constructed by over-specifying the simulated data on the top of the plate while leaving the bottom of the plate with no specified boundary conditions. The edges remained insulated. A time step size of $\Delta t = 0.012\,s$ and a damping parameter $\Lambda = 1.0 \times 10^{-9}$ was used. Figure 6 shows the predicted temperature on the plate bottom for the forward and inverse cases at two different time instances. The average error for the reconstructed temperature field is approximately 1.0%.

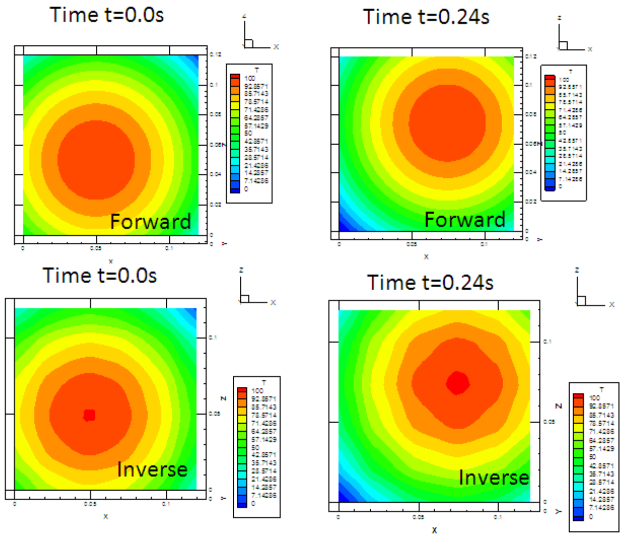

Figure 6. Plate bottom temperatures for forward and inverse cases with no measurement errors.

The above problem was then repeated using over-specified boundary conditions with random measurement errors added. Random errors in the known boundary temperatures and fluxes were generated using the following equations [6]:

$$T = T_{\rm bc} \pm \sqrt{-2\bar{\sigma}^2 \ln R}, \tag{5.2}$$

$$Q = Q_{\rm bc} \pm \sqrt{-2\bar{\sigma}^2 \ln R} \tag{5.3}$$

where R is a uniform random number between 0.0 and 1.0 and $\bar{\sigma}$ is the standard deviation. Equations (5.2)–(5.3) were used to generate errors in both the known boundary heat fluxes and temperatures obtained from the forward solution.

The inverse problem was repeated after random errors were added to the simulated data. The average temperature measurement error in this case is 1.5%. A larger damping parameter of $\Lambda = 6.0 \times 10^{-4}$ was used. A comparison between the inverse and forward temperatures on the bottom surface is shown in Figure 7. Results show that the inverse solution qualitatively matches the forward solution and has an average error in the predicted temperature field of 11%. More regularization is needed to smooth the predicted temperature distribution.

Increasing the damping parameter to $\Lambda = 6.0 \times 10^{-2}$ reduces the average error to 8% and results in a smoother temperature field (Figure 8) compared to the previous case. We note that increasing the parameter further results in an overly smooth temperature field and increased error in the predicted temperature. Therefore, there is an optimal damping parameter for this case, though it is not known *a priori*. The determination of the optimal parameter is a topic for further research.

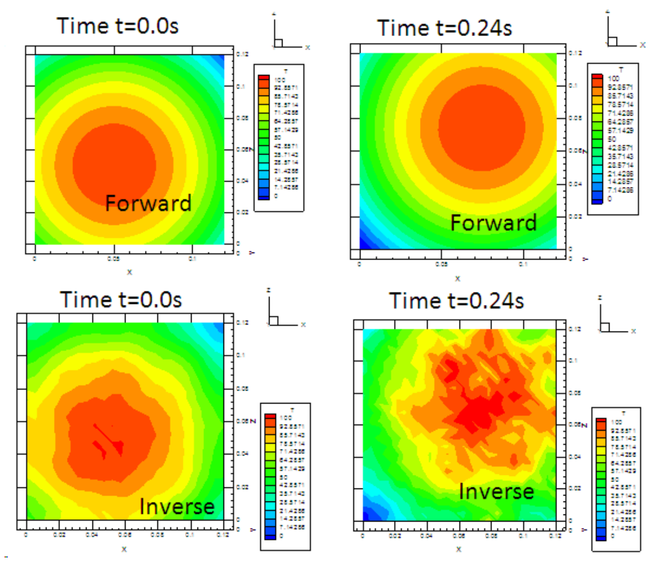

Figure 7. Plate bottom temperatures for forward and inverse cases with 1.5% average measurement error and $\Lambda = 6.0 \times 10^{-4}$.

6 Conclusions

A formulation for the inverse determination of unknown unsteady boundary conditions in heat conduction for three-dimensional problems has been presented. This formulation has been successfully applied to the inverse detection of temperature

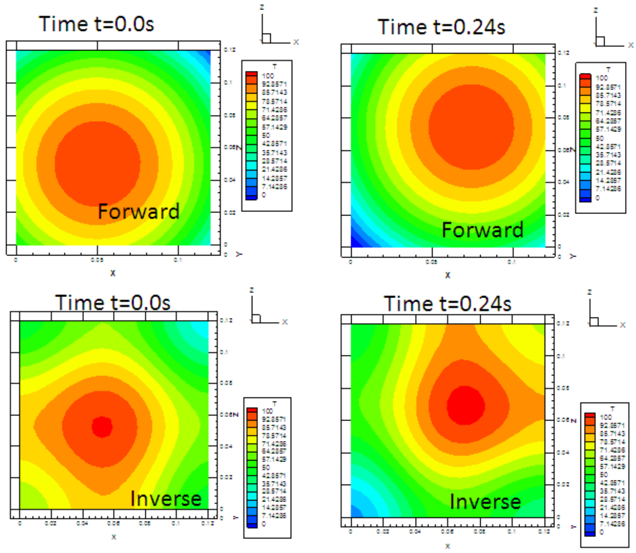

Figure 8. Plate bottom temperatures for forward and inverse cases with 1.5% average measurement error and $\Lambda = 6.0 \times 10^{-2}$.

distributions on inaccessible boundaries for a rod and a plate. Simulated measurements were generated by solving a forward problem with known boundary conditions. This method computes the temperature distribution with high accuracy when no measurement errors were present in the over-specified boundary conditions. This method requires regularization when measurement errors are added to the boundary conditions. However, it was demonstrated that a high-order regularization method successfully prevented the amplification of the errors as a function of time step.

Bibliography

[1] B. H. Dennis and G. S. Dulikravich, Simultaneous determination of temperatures, heat fluxes, deformations, and tractions on inaccessible boundaries, *ASME Journal of Heat Transfer* **121** (1999), 537–545.

[2] B. H. Dennis and G. S. Dulikravich, A 3-D finite element formulation for the determination of unknown boundary conditions in heat conduction, in: *Inverse Problems in Engineering Mechanics III* (Nagano 2001), Eslevier, Amsterdam (2002), 67–76.

[3] B. H. Dennis, G. S. Dulikravich and Z.-X. Han, Determination of temperatures and heat fluxes on surfaces and interfaces of multi-domain three-dimensional electronic components, *ASME Journal of Electronic Packaging* **126** (2004), 457–464.

[4] E. H. Hensel and R. Hills, Steady-state two-dimensional inverse heat conduction, *Numerical Heat Transfer* **15** (1989), 227–240.

[5] M. E. Larsen, An inverse problem: Heat flux and temperature prediction for a high heat flux experiment, Sandia National Laboratories, Tech. Rep. SAND-85-2671, Albuquerque, 1985.

[6] T. J. Martin and G. S. Dulikravich, Inverse determination of boundary conditions in steady heat conduction, *ASME Journal of Heat Transfer* **3** (1996), 546–554.

[7] A. Neumaier, Solving ill-conditioned and singular linear systems: A tutorial on regularization, *SIAM Review* **40** (1998), 636–666.

[8] L. G. Olson and R. D. Throne, The steady inverse heat conduction problem: A comparison for methods of inverse parameter selection, in: *34th National Heat Transfer Conference-NHTC'00*, NHTC2000-12022, Pittsburg, 2000.

[9] C. C. Paige and M. A. Saunders, LSQR: An algorithm for sparse linear equations and sparse least squares, *ACM Transactions on Mathematical Software* **8** (1982), 43–71.

[10] A. N. Tikhonov and V. Y. Arsenin, *Solutions of Ill Posed Problems*, V. H. Wistom and Sons, Washington, 1977.

Received July 24, 2012.

Author information

Brian H. Dennis, Department of Mechanical and Aerospace Engineering,
University of Texas at Arlington, 500 W. First St., Arlington, TX 76019, USA.
E-mail: dennisb@uta.edu

George S. Dulikravich, Department of Mechanical and Materials Engineering,
Florida International University 10555 W. Flagler St., Miami, FL 33174, USA.
E-mail: dulikrav@fiu.edu